Sliding and rolling dissipation in Cosserat plasticity

Granular Matter manuscript No.
(will be inserted by the editor)

Sliding and rolling dissipation in Cosserat plasticity

Stefanos-Aldo Papanicolopulos · Emmanuil Veveakis

Received: date / Accepted: date

Abstract Based on micromechanical considerations at the level of grain contacts and taking into account the way in which kinematic and static quantities are "transported" between grain surface and grain centre, we identify appropriate measures related to energy dissipation due to rolling and sliding between grains, within both a discrete and a Cosserat continuum description.

This allows us, within the framework of Cosserat plasticity, to identify appropriate invariants and formulate simple forms of the respective yield surfaces. The resulting model is shown to be a multiple-yield-surface generalisation of the model by Mühlhaus and Vardoulakis (*Géotechnique*, 1987). By introducing separate and clearly identified rolling- and sliding-resistance parameters, the model allows for separate activation of the respective dissipative mechanisms.

Keywords Cosserat continuum · plasticity · granular micromechanics · sliding · rolling · energy dissipation

1 Introduction

When describing a granular medium, we usually associate each particle with its centre. It is clear, however, that it is at the contacts between particles that all interesting phenomena take place. As stated by Cole & Peters [9] "…the relationship between the contact motions and resisting forces define the micro-scale properties of the medium".

The contact between particles may include both sliding and rolling. Earlier studies of granular media silently assumed that almost all energy dissipation takes place at sliding contacts [26]. Energy dissipation due to rolling cannot however be excluded, e.g. because of micro slip and friction at the contact interface [38]. Indeed, rolling friction plays an important role in different phenomena such as the velocity of landslides [18], the dynamics of sandpile formation [45] and the thickness [7] or evolution [1] of faults.

Oda *et al.* [29] observed that "particle rolling appears to be a major microscopic deformation mechanism, especially when interparticle friction is large". Bardet [2] emphasised that "The rotations of soil particles during laboratory loadings are a well recognized phenomenon in soil mechanics and the micromechanics of granular materials […] However, in modeling the failure for granular materials, the effects of particle rotations have been largely neglected.".

Numerical simulations by Bardet [2] indicate that, in granular media composed of spherical grains, sliding occurs only at a small proportion ($\leq 30\%$) of contacts before plastic yielding, rolling being the bulk amount of contacts. Based on the above considerations, various recent numerical discrete element simulations include energy dissipation due to rolling [21,1,12].

While a discrete description may seem more suitable for modelling granular media, in practical applications a continuum approach may be preferable. In this context, it is usual to consider the application of Cosserat continuum mechanics to the description of the mechanical behaviour of granular media, as pioneered by Oshima [30] and Satake[33], and later Kanatani [22] and Mühlhaus and Vardoulakis [27].

The use of the Cosserat continuum allows describing phenomena that run at the level of individual grains, such as shear-bands occurring within granular bodies [27] or interfacial bands, occurring at shear interfaces between hard, coherent material and granular material [5,39,43]. Considering the complex behaviour exhibited by fully developed shear-bands [41,16] and based on a number of studies [9, 28,2], Vardoulakis [42] proposed the idea of the post-failure

ERC grant agreement n^{o} 228051

S.-A Papanicolopulos · E. Veveakis
Department of Mechanics, National Technical University of Athens
Iroon Polytecniou 5, Zografou 157 73, Greece
E-mail: stefanos@mechan.ntua.gr

activation of a rolling-contact yield mechanism as the main mechanism for strength softening and energy dissipation.

In this paper, we follow the work of Vardoulakis [42] and provide a Cosserat continuum representation of the basic mechanics of granular media, focusing on micromechanical considerations of energy dissipation at grain level, as well as on the concept of "transported" contact quantities. We thus identify the appropriate discrete quantities that should be used to account separately for sliding and rolling at the contacts. By embedding contact quantities in continuum fields and applying a fabric averaging procedure, we then derive appropriate stress invariants that are related to sliding and rolling.

Based on the above, we abandon the single-yield mechanism of interparticle slip [4,27,11] and adopt Lippmann's [24] multi-yield mechanisms idea. This allows us to revisit the plasticity model of Mühlhaus and Vardoulakis [27], by proposing its generalisation as a multiple-surface Cosserat plasticity model that includes separate and clearly identified rolling- and sliding-resistance parameters, thus allowing for separate activation of the respective mechanisms.

2 Cosserat continuum mechanics

Before delving into grain-level considerations, we review here the basic concepts of Cosserat continuum mechanics which will be used when passing from the discrete to the continuum description. We only consider the static case for small deformations, in Cartesian coordinates. Indicial notation is used, with indices i,j,k,l,m ranging from 1 to 3. Repeated indices indicate summation, a comma in the subscripts indicates differentiation, δ_{ij} is the Kronecker delta and e_{ijk} is the permutation tensor.

2.1 Kinematics

The Cosserat continuum is a manifold of oriented rigid particles, called *trièdres rigides* or *rigid crosses* with six degrees of freedom, three of which define the displacement vector u_i and three of which define the rotation vector ψ_i.

As proposed by Schäfer [35], displacements and rotations in the Cosserat continuum can be treated in a unified way using motor algebra and motor calculus [6,35,23,31]. Though this notation leads to simpler expressions and provides a natural way of expressing the concept of transported quantities introduced in Subsection 3.2, it will not be used here as most readers will not be familiar with it.

The deformation measures are the infinitesimal relative deformation tensor γ_{ij} and the infinitesimal tensor of distortions κ_{ij}, defined as

$$\gamma_{ij} = u_{j,i} - e_{ijk}\psi_k, \quad \kappa_{ij} = \psi_{j,i} \tag{1}$$

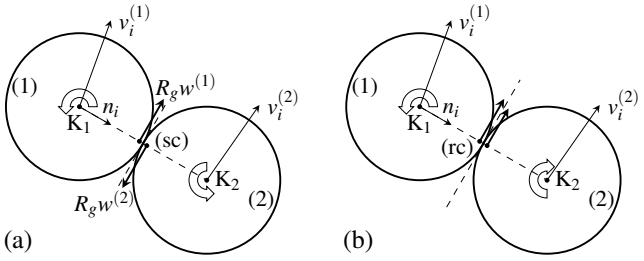

Fig. 1 Two-grain circuit with (a) sliding contact and (b) rolling contact respectively.

where the symmetric part of γ_{ij} is the strain, the antisymmetric part is the relative rotation, the diagonal terms of κ_{ij} are the torsions and the off-diagonal terms are the curvatures.

The rate of displacement and of rotation is respectively the velocity v_i and the spin w_i. The "rate of relative deformation" and "rate of distortion" tensors are then given by

$$\Gamma_{ij} = v_{j,i} - e_{ijk}w_k, \quad K_{ij} = w_{j,i} \tag{2}$$

2.2 Statics

The relative deformation is energy-conjugate to the stress σ_{ij}, while the distortion is energy-conjugate to the couple stress μ_{ij}. The power of the internal forces (per unit volume) for the Cosserat continuum is thus given by ([44], pp. 340)

$$P = \sigma_{ij}\Gamma_{ij} + \mu_{ij}K_{ij} \tag{3}$$

In the classical continuum, the only static quantity is the stress σ_{ij}, which is symmetric, so an isotropic yield function would be a function of the 3 stress invariants. In the Cosserat continuum, neither σ_{ij} nor μ_{ij} is symmetric. There are therefore 39 independent invariants of σ_{ij} and μ_{ij} in three dimensions ([20], p. 114), which can be written as polynomials of the stress and couple-stress components. For example there are 8 invariants of order up to two (σ_{ii}, μ_{ii}, $\sigma_{ij}\sigma_{ji}$, $\sigma_{ij}\sigma_{ij}$, $\mu_{ij}\mu_{ji}$, $\mu_{ij}\mu_{ij}$, $\sigma_{ij}\mu_{ji}$, $\sigma_{ij}\mu_{ij}$). In the following, we use micromechanical considerations to determine the appropriate invariants to use for Cosserat plasticity.

3 Intergranular dissipation

Consider the contact of two rotating grains in Figure 1. Homothetical rotation results in strong contact sliding and weak contact rolling, while antithetical rotation results in weak contact sliding and strong contact rolling.

Note that we consider the grains to be spheres (and draw them as discs for simplicity), therefore keeping only information about the position of the centre of the particle and the contact point. The fact that the grains in reality have arbitrary shapes is however reflected in the presence of contact couples [14].

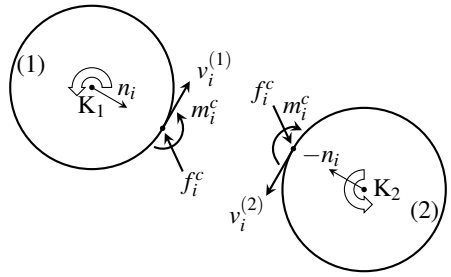

Fig. 2 Contact forces and contact couples between grains

3.1 Grain contact energetics

Consider either pair of grains in Figure 1. Assuming that both grains have the same radius R_g, the branch vector connecting the centres of the two grains is

$$(\mathrm{K}_2-\mathrm{K}_1)_i = 2\ell_i \quad \text{with} \quad \ell_i = R_g n_i \tag{4}$$

where n_i is the unit vector normal to the contact plane and pointing towards grain (2).

The centres of the grains, points K_1 and K_2, move with velocities $v_i^{(1)}$ and $v_i^{(2)}$, while the grains rotate with angular velocities $w_i^{(1)}$ and $w_i^{(2)}$, respectively. At the contact, the velocities of the grains are

$$v_i^{(1)c} = v_i^{(1)} + e_{ilk} w_l^{(1)} \ell_k, \qquad v_i^{(2)c} = v_i^{(2)} - e_{ilk} w_l^{(2)} \ell_k \tag{5}$$

therefore the relative rotation and relative velocity of grain (2) with respect to grain (1) at the contact point are

$$w_i^{(2,1)c} = w_i^{(2)} - w_i^{(1)} \tag{6}$$

$$v_i^{(2,1)c} = v_i^{(2)c} - v_i^{(1)c} = v_i^{(2)} - v_i^{(1)} - e_{ijk}(w_j^{(2)} + w_j^{(1)})\ell_k \tag{7}$$

The two grains interact through contact forces and contact couples. As shown in Figure 2, the force $f_i^{(2,1)c} = f_i^c$ and couple $m_i^{(1,2)c} = m_i^c$ are applied on grain (2) by grain (1), while their equal and opposite reactions $f_i^{(1,2)c}$ and $m_i^{(1,2)c}$ are applied on grain (1) by grain(2). The power of the contact forces per unit volume (due to sliding) is

$$\begin{aligned} P^{(ns)} &= \tfrac{1}{V}\left(f_i^{(2,1)c} v_i^{(2)c} + f_i^{(1,2)c} v_i^{(1)c}\right) \\ &= \tfrac{1}{V} f_i^{(2,1)c}(v_i^{(2)c} - v_i^{(1)c}) = \tfrac{1}{V} f_i^{(2,1)c} v_i^{(2,1)c} \end{aligned} \tag{8}$$

while the power of the couples (due to rolling) is

$$\begin{aligned} P^{(nr)} &= \tfrac{1}{V}(m_i^{(2,1)c} w_i^{(2)} + m_i^{(1,2)c} w_i^{(1)}) \\ &= \tfrac{1}{V} m_i^{(2,1)c}(w_i^{(2)} - w_i^{(2)}) = \tfrac{1}{V} m_i^{(2,1)c} w_i^{(2,1)} \end{aligned} \tag{9}$$

The reference volume V is not specified here, but is left as a free parameter.

The total power of actions at grain contact is the sum of the contributions due to sliding and rolling

$$P^{(n)} = P^{(ns)} + P^{(nr)} \tag{10}$$

3.2 Continuum embedment

To pass from the discrete to the continuum description, we use a "continuum embedment" procedure, that is we assume that the particle spin and velocity are embedded into continuous fields. This allows us to linearise these fields around the contact point to obtain

$$w_i^{(1)} = w_i^c - \ell_m w_{i,m}^c, \qquad w_i^{(2)} = w_i^c + \ell_m w_{i,m}^c \tag{11}$$

$$v_i^{(1)} = v_i^c - \ell_m v_{i,m}^c, \qquad v_i^{(2)} = v_i^c + \ell_m v_{i,m}^c \tag{12}$$

Using equations (6), (7) and (2), we finally get

$$w_i^{(2,1)c} = w_i^{(2)} - w_i^{(1)} = 2\ell_m w_{i,m}^c = 2\ell_m K_{mi}^c \tag{13}$$

$$\begin{aligned} v_i^{(2,1)c} &= v_i^{(2)} - v_i^{(1)} - e_{ijk}(w_j^{(2)} + w_j^{(1)})\ell_k \\ &= 2\ell_m(v_{i,m}^c - e_{ijm} w_j^c) = 2\ell_m \Gamma_{mi}^c \end{aligned} \tag{14}$$

thus the relative spin and velocity can be expressed in terms of the related Cosserat-continuum deformation measures.

We assume that the force f_i and couple m_i are generated by a continuous stress field and couple stress field, respectively, evaluated at the contact between the considered grains. Thus

$$f_i^{(2,1)c} = \sigma_{ki}^c n_k S, \qquad m_i^{(2,1)c} = \mu_{ki}^c n_k S \tag{15}$$

where S is a reference surface area, left unspecified like the reference volume V. Equations (8) and (9) then result in

$$P^{(ns)} = (2R_g S/V) n_k n_m \sigma_{ki}^c \Gamma_{mi}^c \tag{16}$$

$$P^{(nr)} = (2R_g S/V) n_k n_m \mu_{ki}^c K_{mi}^c \tag{17}$$

so that

$$P^{(n)} = (2R_g S/V) n_k n_m (\sigma_{ki}^c \Gamma_{mi}^c + \mu_{ki}^c K_{mi}^c) \tag{18}$$

The material point, however, is usually considered to be centred on the centre of the particle. We therefore consider the power of contact forces and couples using as reference point the centre of particle (1). The kinematic quantities at the contact are calculated as

$$w_i^{(2,1)c} = 2\ell_m K_{mi}^{(1)}, \qquad v_i^{(2,1)c} = 2\ell_m(\Gamma_{mi}^{(1)} + e_{ikl}\ell_k K_{ml}^{(1)}) \tag{19}$$

Comparison with equations (13) and (14) yields

$$K_{mi}^c = K_{mi}^{(1)}, \quad \Gamma_{mi}^c = \Gamma_{mi}^{(1)} + e_{ikl}\ell_k K_{ml}^{(1)} \tag{20}$$

The stress and couple stress at the contact are calculated as

$$\sigma_{ij}^c = \sigma_{ij}^{(1)}, \qquad \mu_{ij}^c = \mu_{ij}^{(1)} + e_{jlk}\ell_l \sigma_{ik}^{(1)} \tag{21}$$

where $\sigma_{ij}^{(1)}$ and $\mu_{ij}^{(1)}$ are the stress and couple stress evaluated at the centre of particle (1). This leads to

$$P^{(ns)} = (2R_g S/V)\, n_k n_j\, \sigma_{ki}^{(1)} (\Gamma_{ji}^{(1)} + e_{imn}\ell_m K_{jn}^{(1)}) \tag{22}$$

$$P^{(nr)} = (2R_g S/V)\, n_k n_j\, (\mu_{ki}^{(1)} + e_{imn}\ell_m \sigma_{kn}^{(1)}) K_{ji}^{(1)} \tag{23}$$

and finally to

$$P^{(n)} = (2R_g S/V)\, n_k n_j\, (\sigma_{ki}^{(1)} \Gamma_{ji}^{(1)} + \mu_{ki}^{(1)} K_{ji}^{(1)}) \tag{24}$$

Equations (20) and (21) give the so-called "transported contact quantities", that is the kinematic and static quantities at the contact point calculated based on the respective values at the particle centre.

We note that the final expressions for $P^{(n)}$ are the same, independently of the location at which we evaluate the kinematic and static quantities. When evaluating separately the sliding and rolling contributions, however, it is necessary to consider the transported contact quantities.

3.3 Fabric averaging

Equations (20) to (24) refer to quantities that still depend on the normal to the contact n_i. To obtain useful continuum fields, we eliminate the dependence on n_i by taking into account the distribution of the contacts, that is the fabric of the granular medium. This is done by computing a "fabric average" of quantities over the surface of the grain.

To compute the average $\langle\cdot\rangle$ of a contact quantity (such as $P^{(n)}$) over the surface of a grain, we need to specify a probability distribution of the unit contact normals n_i. We use here for simplicity a uniform distribution, though more realistic modelling requires more complex distributions [26, 34].

It can be easily shown that [22]

$$\langle n_i n_j \rangle = \tfrac{1}{3}\delta_{ij} \tag{25}$$

$$\langle n_i n_j n_k n_l \rangle = \tfrac{1}{3}(\delta_{ij}\delta_{kl} + \delta_{ik}\delta_{jl} + \delta_{il}\delta_{jk}) \tag{26}$$

while the average of the product of an odd number of unit vectors is zero.

The average power of contact forces and couples, given either by equation (18) or by (24), is therefore

$$\langle P^{(n)} \rangle = (2R_g S/3V)(\sigma_{ji}\Gamma_{ji} + \mu_{ji} K_{ji}) \tag{27}$$

By setting $2R_g S = 3V$ we obtain

$$\langle P^{(n)} \rangle = P \tag{28}$$

where P is the power of internal actions in the Cosserat continuum given in equation (3).

With this specific choice of micromechanical variables at the level of intergranular contact, the stress power of the Cosserat continuum is therefore calculated as the isotropic average value of the work done by contact forces and contact couples.

3.4 Stress and couple-stress invariants

We decompose the stress tensor into a spherical and a deviatoric part

$$\sigma_{ij} = s_{ij} + p\delta_{ij} \quad \text{with} \quad p = \tfrac{1}{3}\sigma_{kk} \tag{29}$$

and then decompose the stress vector $t_i = \sigma_{ki} n_k$ into a normal component

$$t^{(n)} = t_i n_i = \sigma_{ki} n_k n_i = (s_{ki} + p\delta_{ki}) n_k n_i \tag{30}$$

and a shear (i.e. tangential) component

$$t_i^{(t)} = t_i - t^{(n)} n_i = \sigma_{kl} n_k (\delta_{il} - n_i n_l) = s_{kl} n_k (\delta_{il} - n_i n_l) \tag{31}$$

This decomposition allows the calculation of the following stress invariants: the mean normal traction on contact

$$\langle t^{(n)} \rangle = p \tag{32}$$

and the mean of the square of the magnitude of the shear traction on contacts

$$T^2 = \langle t_k^{(t)} t_k^{(t)} \rangle = \tfrac{4}{15} s_{ij} s_{ij} - \tfrac{1}{15} s_{ij} s_{ji} \tag{33}$$

Similarly, the couple stress can be decomposed as

$$\mu_{ij} = c_{ij} + \mu_\tau \delta_{ij} \quad \text{with} \quad \mu_\tau = \tfrac{1}{3}\mu_{kk} \tag{34}$$

while the couple-stress vector $m_i = \mu_{ki} n_k$ can be decomposed into a normal component $m^{(n)}$ and a tangential component $m_i^{(t)}$, giving the invariants

$$\langle m^{(n)} \rangle = \mu_\tau \tag{35}$$

and

$$M^2 = \langle m_k^{(t)} m_k^{(t)} \rangle = \tfrac{4}{15} c_{ij} c_{ij} - \tfrac{1}{15} c_{ij} c_{ji} \tag{36}$$

Following Section 3.2, however, the invariants related to rolling must be calculated using the transported couple stress. We therefore obtain, after a few calculations,

$$\langle m^{(n)c} \rangle = \langle m^{(n)} \rangle \tag{37}$$

and

$$\langle m_i^{(t)c} m_i^{(t)c} \rangle = \langle m_i^{(t)} m_i^{(t)} \rangle + R_g^2 \langle t_i^{(t)} t_i^{(t)} \rangle \tag{38}$$

that is,

$$(M^c)^2 = M^2 + R_g^2 T^2 \tag{39}$$

Together with p, the invariants T, μ_τ and M^c can be used to formulate simple plasticity-based constitutive equations for granular media that account for dissipation due to grain sliding, torsion and rolling respectively.

4 A two-dimensional Cosserat plasticity model

Considering only the simplified case of a two-dimensional continuum, we present here a plasticity model based on the micromechanical considerations of Section 3.

4.1 Two-dimensional invariants

The invariants presented in Section 3.4 assume a different form in two dimensions

$$p = \tfrac{1}{2}(\sigma_{11} + \sigma_{22}) \tag{40}$$

$$T^2 = \tfrac{1}{4}(s_{11}^2 + s_{22}^2 + s_{12}^2 + s_{21}^2) + \tfrac{1}{8}(s_{12} - s_{21})^2 \tag{41}$$

$$\mu_\tau = 0 \tag{42}$$

$$M^2 = \tfrac{1}{2}(\mu_{13}^2 + \mu_{23}^2) \tag{43}$$

while equation (39) still holds

$$(M^c)^2 = M^2 + R_g^2 T^2 \tag{44}$$

Introducing the invariants of the deviatoric symmetric and the antisymmetric stress

$$q^2 = \tfrac{1}{4}(s_{11} - s_{22})^2 + \tfrac{1}{4}(s_{12} + s_{21})^2, \quad r = \tfrac{1}{2}|s_{12} - s_{21}| \tag{45}$$

the invariant T can be written as

$$T^2 = \tfrac{1}{2}q^2 + r^2 \tag{46}$$

4.2 Yield surface for sliding

Section 3 shows that sliding is related to the stress σ_{ij}, therefore the yield surface for sliding should depend on the invariants of σ_{ij}. Specifically, following the discussion in Section 3.4, the simplest yield surface for sliding would be

$$F_1 = \sqrt{2}T + f_s p = \sqrt{q^2 + 2r^2} + f_s p \tag{47}$$

where f_s is a sliding resistance.

Another possibility is to use the Mohr-Coulomb criterion, which states that

$$|t^{(t)}| \leqslant -t^{(n)} \tan\phi \tag{48}$$

where $|t^{(t)}|$ is the magnitude of the shear component of the stress vector $t_i^{(t)}$, $t^{(n)}$ is the normal component of the stress vector for a given orientation n_i and ϕ is a friction angle.

As shown by Satake [33] and presented in more detail by other authors [10, 19, 13], the locus of the normal and shear components of the stress vector for all possible orientations is a (Mohr) circle whose centre does not lie on the axis of zero shear stress. This is shown in Figure 3, where it can be shown that $\overline{\mathrm{AM}} = r$, $\overline{\mathrm{MC}} = q$, $\overline{\mathrm{OA}} = -p$, so that the yield surface can be written as

$$F_1^* = q + r\cos\phi + p\sin\phi \tag{49}$$

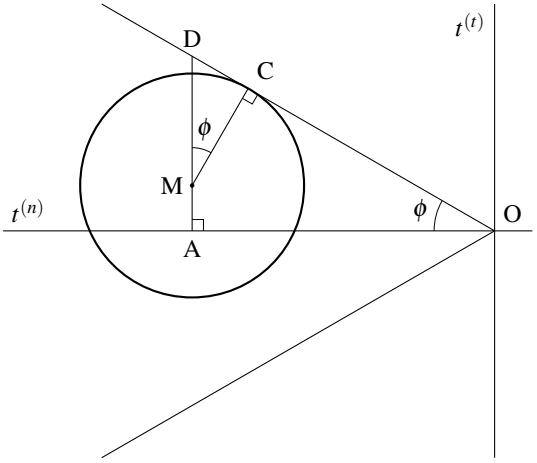

Fig. 3 Mohr's circle for asymmetric two-dimensional stress.

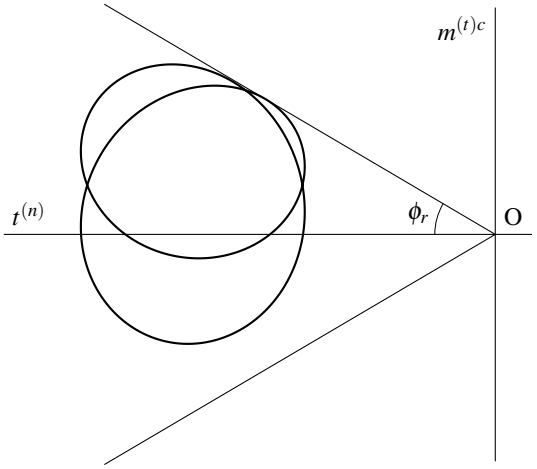

Fig. 4 Example of a $m^{(t)c}$ versus $t^{(n)}$ curve together with the yield envelope for rolling.

4.3 Yield surface for rolling

The yield surface for rolling should depend on the invariants of μ_{ij}^c. The simplest such surface would be

$$\begin{aligned} F_2 &= (\sqrt{2}/R_g)M^c + f_r p \\ &= \sqrt{2(M/R_g)^2 + q^2 + 2r^2} + f_r p \end{aligned} \tag{50}$$

where f_r is a rolling resistance.

It is also possible to consider a "maximum value" criterion, as in the Mohr-Coulomb criterion in equation (48), which states that

$$|m^{(t)c}|/R_g \leqslant -t^{(n)} \tan\phi_r \tag{51}$$

However the resulting yield surface is more difficult to formulate, since the $m^{(t)c}$ versus $t^{(n)}$ curve is not a circle, as shown in Figure 4.

5 Comparison with the Mühlhaus–Vardoulakis model

In their seminal paper, Mühlhaus and Vardoulakis [27] introduced a single-surface two-dimensional Cosserat plasticity model (called here the MV model). The yield surface of the MV model is

$$F_{MV} = \bar{\tau} + f_g p \tag{52}$$

where $\bar{\tau}$ is a "generalised" shear stress intensity and f_g is a resistance parameter. With the notation used in this paper, $\bar{\tau}$ can be written as

$$\bar{\tau}^2 = q^2 + \xi r^2 + 2(M/R_g)^2 \tag{53}$$

where $\xi = 2$ for the so-called "static" model and $\xi = 1/2$ for the "kinematical" model [44].

We notice that, when $f_g = f_r$, the yield surface for the "static" MV model coincides with the rolling-related yield surface F_2 for the present model, given in equation (50). We therefore consider the MV model as a rolling-resistance model, though it is expressed in terms of a "stress" invariant.

Comparing the yield surfaces F_1 and F_2 it is easily seen that if $f_r \leqslant f_s$ then $F_2 \geqslant F_1$, in which case the F_2 surface is always reached first, so the model degenerates into a single-surface one, which is actually the MV model. In this sense, the present framework represents a generalisation of the MV model, allowing for (but not necessarily requiring) the separate activation of sliding- and rolling-related resistance. As it is expected that at the onset of plastic yield the relation $f_r \leqslant f_s$ will hold, we can consider the rolling-related mechanism as the principal mechanism of energy dissipation.

Based on the above considerations, it is clear that a localisation analysis using the proposed model will agree with previous analyses using the MV model [27,44], as far as the onset of localisation is concerned. An example of such an analysis for a simple case is given in Section 6. The direction along which the shear band will develop will also be the same, as determined by the zero value of the determinant of the acoustic tensor [40].

The determination of the evolution of the shear band, however, may differ from previous analyses, depending critically on the evolution law for the rolling resistance of the material. Also at issue is the determination of the proper conditions at the shear band boundary based on the proposed micromechanical considerations, as two different conditions have been proposed in the literature [27,3,37].

6 Application to a simple shear problem

We may apply the model presented in Section 4 to the problem of simple shear of an infinite, thick slab of a Cosserat continuum (Fig. 5a), in order to study the conditions of the material at incipient failure. As discussed previously, the rolling surface is the one assumed to be reached first, being responsible for the onset of plastic yielding.

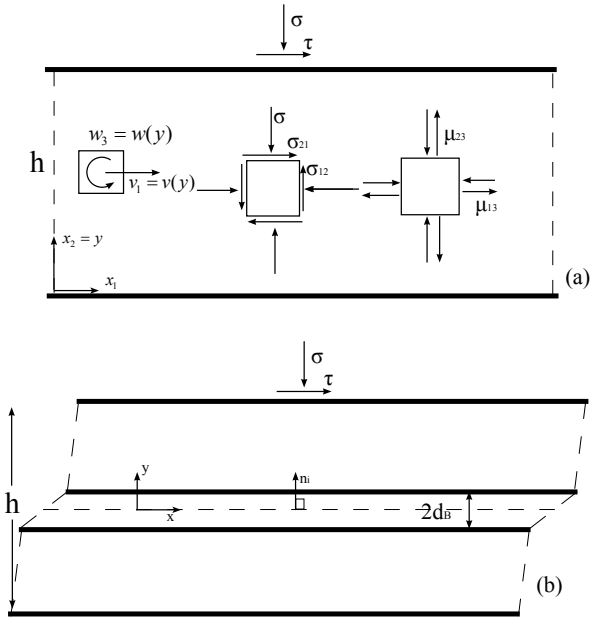

Fig. 5 Simple shear of an infinite slab of Cosserat continuum. (a) Stresses and couple stresses (b) Shear band formation at the onset of plasticity.

The analysis is briefly presented in Appendix A, where the shear band thickness at incipient failure (Fig. 5b) is estimated as

$$\frac{d_B}{R_g} = \frac{\pi}{A} \quad \text{with} \quad A = \sqrt{\frac{16 f_r^2 (1+2f_r^2)}{1+8f_r^2(1+3f_r^2)}} \tag{54}$$

We may plot the solution (54) against the rolling resistance f_r (Fig. 6), to notice what intuitively one would expect from continua with microstructure: In materials with strong rolling resistance (like sand or gouge materials) the shear band thickness decreases, in accordance with classical experimental [27] and recent DEM results on sands [15], and field evidence on faults [8]. On the other extreme, at the limit of no rolling resistance, $f_r \to 0$ no shear band is formed, as $d_B \to \infty$. Thus continua with no internal rolling mechanisms, like for example Newtonian fluids, will not present any localisation of the deformation, in accordance with the experimental observations of fluid mechanics.

The present study ceases to be valid after the continuous bifurcation that marks the incipient failure of the material (see Appendix A). Past this point, sliding contacts increase rapidly [2], triggering the sliding yield surface. As mentioned in Section 5, in order to extend the validity of the model in the post-failure regime, additional information is needed on the evolution of sliding and rolling resistance parameters of the material, as well as the proper conditions for the stresses and couple stresses at the shear band boundary.

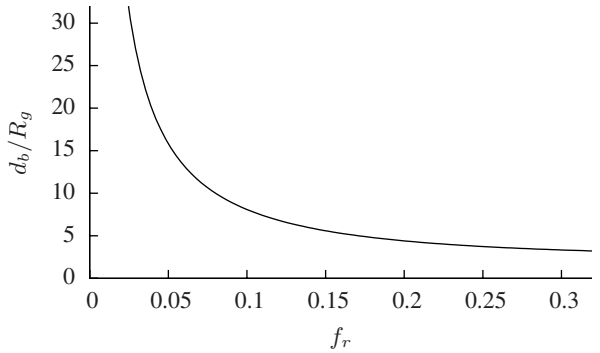

Fig. 6 Shear band thickness versus rolling resistance, plotted from equation (54).

7 Conclusions

Based on micromechanical considerations, our analysis provides a starting point for the identification of appropriate kinematic and static quantities to be used in the description of energy dissipation mechanisms due to rolling and sliding. A central issue in this analysis is the identification of different continuum quantities at the centres of grains and at their contacts, together with the use of appropriate transport laws.

The simplest possible model resulting from this analysis is a two-dimensional multi-surface plasticity Cosserat model with two independent resistance parameters to separately account for sliding and rolling mechanism. This model can be seen as a generalisation of the model proposed by Mühlhaus and Vardoulakis.

The framework we presented is appropriate for the study of the different energy dissipation mechanisms in granular materials. Appropriate experimental evidence is needed, however, to determine the initial values and the evolution laws for the two different resistance parameters. Additionally, the yield surfaces given here must be related to appropriate plastic flow rules to account for kinematic effects such as stress dilatancy.

Acknowledgements The research leading to these results has received funding from the European Research Council under the European Community's Seventh Framework Programme (FP7/2007–2013) — ERC grant agreement n^{o} 228051 [MEDIGRA].

A Bifurcation analysis at incipient failure

In the absence of any other information concerning the plastic potential of the rolling mechanism, we assume associative plasticity for the second yield surface. The corresponding rate equations for the stresses and couple stresses admit the form $\dot{\sigma}_{ij} = D^{(ep)}_{ijkl}\dot{\Gamma}_{kl}$ and $\dot{\mu}_{i3} = M^{(ep)}_{ij}K_{j3}$, where

$$D^{(ep)}_{ijkl} = D^{(e)}_{ijkl} - <1> \frac{D^{(e)}_{ijab}Q_{ab}Q_{ij}D^{(e)}_{ijkl}}{Q_{ij}D^{(e)}_{ijkl}Q_{kl} + F_i M^{(ep)}_{ij}F_j + h2} \tag{55}$$

$$M^{(ep)}_{ij} = M^{(e)}_{ij} - <1> \frac{M^{(e)}_{ij}F_k F_l M^{(e)}_{lj}}{F_i M^{(e)}_{ij}F_j + h_2} \tag{56}$$

where $Q_{ij} = \frac{\partial F_2}{\partial \sigma_{ij}}$, $F_i = \frac{\partial F_2}{\partial \mu_{i3}}$, F_2 being the yield surface of rolling, Eq. (50). The elasticity matrices are defined as $M^{(el)}_{ij} = 4GR_g^2\delta_{ij}$ and

$$\mathbf{D^{(el)}} = G\begin{pmatrix} K+1 & K-1 & 0 & 0 \\ K-1 & K+1 & 0 & 0 \\ 0 & 0 & 1+h^C & 1-h^C \\ 0 & 0 & 1-h^C & 1+h^C \end{pmatrix} \tag{57}$$

where $h^C = G^C/G = 1/2$ is the Cosserat shear modulus, as described in [44], h_2 the hardening modulus of the second yield surface and $K = 1/(1-2\nu)$ the normalised bulk modulus.

In order to demonstrate the main aspects of the presented model we assume for simplicity the simple shear problem of an infinite slab of Cosserat continuum, whose thickness is also infinite compared to the characteristic Cosserat length R_g (Fig. 5a). In this case all mechanical fields are assumed to vary along the x_2-axis.

Since we study the onset of plastic yielding, the problem consists in studying whether the constitutive description admits a solution that corresponds to a continuous-to-discontinuous bifurcation in the form of a planar shear-band, in the lines of the Tomas-Hill-Mandel model [36,17,25]. From the nullity of the determinant of the acoustic tensor $|D^{(ep)}_{ijkl}n_j n_l| = 0$ we may determine the direction of that shear band $\theta_B = \arctan(-n_1/n_2) = 0$ (n_i being the unit vector normal to the shear band, Fig 5b), obtaining as expected a horizontal one. From the same criterion (see [32]) we may calculate the critical hardening modulus at the onset of instability, $h_2 = 0$, as expected from the assumption of associativity. In this model however, apart from the acoustic tensor, we also deduce the tensor $B = M^{(ep)}_{ij}n_i n_j$ which in the classical continuum (where $R_g = 0$) does not exist. The determinant of this tensor is always positive in the specific problem under study, yielding that both the spin and the rate curvature deformation are continuous across the shear band at first bifurcation.

We may implement the above rate equations in the governing equilibrium equations ([44], pp. 344),

$$\frac{\partial \dot{\sigma}_{21}}{\partial y} = 0 \Rightarrow \sigma_{21} = \tau = const., \tag{58}$$

$$\frac{\partial \dot{\sigma}_{22}}{\partial y} = 0 \Rightarrow \sigma_{22} = \sigma = const., \tag{59}$$

$$\frac{\partial \dot{\mu}_{23}}{\partial y} + \dot{\sigma}_{21} - \dot{\sigma}_{12} = 0 \Rightarrow w_3''(y) + A^2 w_3(y) = 0 \tag{60}$$

where

$$A^2 = 4\frac{D^{(EP)}_{3222}D^{(EP)}_{4421} - D^{(EP)}_{3421}D^{(EP)}_{4222}}{D^{(EP)}_{4222} + D^{(EP)}_{4421}} \tag{61}$$

By applying the appropriate boundary conditions ($\mu_{23} = 0$ at $x_2 = \pm d_B$, see also [44], pp. 358), we may estimate the shear band thickness at incipient failure as

$$\frac{d_B}{R_g} = \frac{\pi}{A} \tag{62}$$

References

1. Alonso-Marroquín, F., Vardoulakis, I., Herrmann, H.J., Weatherley, D., Mora, P.: Effect of rolling on dissipation in fault gouges. Phys. Rev. E **74**(3), 031,306 (2006)
2. Bardet, J.P.: Observations on the effects of particle rotations on the failure of idealized granular materials. Mech. Mater. **18**(2), 159–182 (1994). Special Issue on Microstructure and Strain Localization in Geomaterials
3. Bardet, J.P., Proubet, J.: Numerical investigation of the structure of persistent shear bands in granular media. Géotechnique **41**(4), 599–613 (1991)
4. Besdo, D.: Ein Beitrag zur nichtlinearen Theorie des Cosserat-Kontinuums. Acta Mech. **20**(1), 105–131 (1974)
5. Bogdanova-Bontcheva, N., Lippmann, H.: Rotationssymmetrisches ebenes Fließen eines granularen Modellmaterials. Acta Mech. **21**(1), 93–113 (1975)
6. Brand, L.: Vector and Tensor Analysis. John Wiley (1947)
7. Chambon, G., Schmittbuhl, J., Corfdir, A., Orellana, N., Diraison, M., Géraud, Y.: The thickness of faults: From laboratory experiments to field scale observations. Tectonophysics **426**(1-2), 77 – 94 (2006)
8. Chester, F.M., Chester, J.S.: Ultracataclasite structure and friction processes of the punchbowl fault, san andreas system, california. Tectonophysics **295**(1-2), 199 – 221 (1998)
9. Cole, D.M., Peters, J.F.: A physically based approach to granular media mechanics: grain-scale experiments, initial results and implications to numerical modeling. Granul. Matter **9**(5), 309–321 (2007)
10. De Paor, D.G.: The role of asymmetry in the formation of structures. J. Struct. Geol. **16**(4), 467 – 475 (1994)
11. Dietsche, A., Willam, K.: Boundary effects in elasto-plastic Cosserat continua. Int. J. Solids Struct. **34**(7), 877–893 (1997)
12. Estrada, N., Taboada, A., Radjaï, F.: Shear strength and force transmission in granular media with rolling resistance. Phys. Rev. E **78**(2), 021,301 (2008)
13. de Figueiredo, R.P., do A. Vargas, E., Moraes, A.: Analysis of bookshelf mechanisms using the mechanics of Cosserat generalized continua. J. Struct. Geol. **26**(10), 1931 – 1943 (2004)
14. Froiio, F., Tomassetti, G., Vardoulakis, I.: Mechanics of granular materials: The discrete and the continuum descriptions juxtaposed. Int. J. Solids Struct. **43**(25-26), 7684–7720 (2006)
15. Gerolymatou, E., Froiio, F., Nouguier-Lehon, C.: Energy-rates for granular materials; discrete characterization. In: 9th HSTAM International Congress on Mechanics, Limassol, Cyprus, pp. 169–175 (2010)
16. Gutiérrez, M., Vardoulakis, I.: Energy dissipation and post-bifurcation behaviour of granular soils. Int. J. Numer. Anal. Methods Geomech. **31**(3), 435–455 (2007)
17. Hill, R.: Acceleration waves in solids. J. Mech. Phys. Solids **10**(1), 1–16 (1962)
18. Huang, R.Q., Wang, S.T.: Rolling friction mechanism for high speed motion of a landslide. In: C. Bonnard (ed.) Proceedings of the 5th International Symposium on Landslides, pp. 187–191. Lausanne (1998)
19. Iordache, M.M., Willam, K.: Localized failure analysis in elasto-plastic Cosserat continua. Comput. Methods Appl. Mech. Eng. **151**(3-4), 559 – 586 (1998)
20. Itskov, M.: Tensor algebra and tensor analysis for engineers with applications to continuum mechanics. Springer-Verlag, Berlin, Heidelberg, New York (2007)
21. Jiang, M., Yu, H.S., Harris, D.: A novel discrete model for granular material incorporating rolling resistance. Comput. Geotech. **32**(5), 340–357 (2005)
22. Kanatani, K.I.: A micropolar continuum theory for the flow of granular materials. Int. J. Eng. Sci. **17**(4), 419–432 (1979)
23. Kessel, S.: Stress functions and loading singularities for the infinitely extended linear elastic-isotropic Cosserat continuum. In: E. Kröner (ed.) Mechanics of Generalized Continua, pp. 114–119. Springer (1968)
24. Lippmann, H.: Eine Cosserat-Theorie des plastischen Fließens. Acta Mech. **8**(3), 255–284 (1969)
25. Mandel, J.: Ondes plastiques dans un milieu indéfini à trois dimensions. J. Méchanique **1**, 3–30 (1962)
26. Mehrabadi, M.M., Cowin, S.C.: Initial planar deformation of dilatant granular materials. J. Mech. Phys. Solids **26**(4), 269–284 (1978)
27. Mühlhaus, H.B., Vardoulakis, I.: The thickness of shear bands in granular materials. Géotechnique **37**(3), 271–283 (1987)
28. Oda, M., Kazama, H..: Microstructure of shear bands and its relation to the mechanisms of dilatancy and failure of dense granular soils. Géotechnique **48**(4), 465–481 (1998)
29. Oda, M., Konishi, J., Nemat-Nasser, S.: Experimental micromechanical evaluation of strength of granular materials: Effects of particle rolling. Mech. Mater. **1**(4), 269–283 (1982)
30. Oshima, N.: Dynamics of granular media. In: K. Kondo (ed.) Memoirs of the Unifying Study of the Basic Problems in Engineering Sciencs by means of Geometry, vol. Vol. 1, Division D, pp. 563–572. Gakujutsu Bunken Fukyo-Kai (1955)
31. Povstenko, Y.Z.: Analysis of motor fields in Cosserat continua of two and one dimensions and its applications. ZAMM J. Appl. Math. Mech. **66**(10), 505–507 (1986)
32. Rudnicki, J.W., Rice, J.R.: Conditions for the localization of deformation in pressure-sensitive dilatant materials. J. Mech. Phys. Solids **23**, 371–394 (1975)
33. Satake, M.: Some considerations on the mechanics of granular materials. In: E. Kröner (ed.) Mechanics of Generalized Continua, pp. 156–159. Springer (1968)
34. Satake, M.: Fabric tensor in granular materials. In: IUTAM Conference on Deformation and Failure of Granular Materials, pp. 63–68. Balkema (1982)
35. Schäfer, H.: Analysis der Motorfelder im Cosserat-Kontinuum. ZAMM Z. Angew. Math. Mech. **47**(5), 319–328 (1967)
36. Thomas, T.Y.: Plastic Flow and Fracture, vol. 2. Academic Press (1961)
37. Tordesillas, A., Peters, J.F., Gardiner, B.S.: Shear band evolution and accumulated microstructural development in Cosserat media. Int. J. Numer. Anal. Methods Geomech. **28**(10), 981–1010 (2004)
38. Tordesillas, A., Walsh, D.C.S.: Incorporating rolling resistance and contact anisotropy in micromechanical models of granular media. Powder Technol. **124**(1-2), 106–111 (2002)
39. Unterreiner, F., Vardoulakis, I.: Interfacial localisation in granular media. In: H.J. Siriwardane, M.M. Zaman (eds.) Computer Methods in Geomechanics. Balkema (1994)
40. Vardoulakis, I.: Shear band inclination and shear modulus of sand in biaxial tests. Int. J. Numer. Anal. Methods Geomech. **4**(2), 103–119 (1980)
41. Vardoulakis, I., Georgopoulos, I.O.: The stress-dilatancy hypothesis revisited: shear-banding related instabilities. Soils Found. **45**(2), 61–76 (2005)
42. Vardoulakis, I., Gerolymatou, E., Papanicolopulos, S.A.: On the Cosserat structure of the micromechanics of granular materials. MEDIGRA project internal report, National Technical University of Athens (2009)
43. Vardoulakis, I., Shah, K., Papanastasiou, P.: Modelling of tool-rock shear interfaces using gradient-dependent flow theory of plasticity. Int J. Rock Mech. Min. Sci. Geomech. Abstr. **29**(6), 573–582 (1992)
44. Vardoulakis, I., Sulem, J.: Bifurcation Analysis in Geomechanics. Blackie Academic & Professional (1995)
45. Zhou, Y.C., Wright, B.D., Yang, R.Y., Xu, B.H., Yu, A.B.: Rolling friction in the dynamic simulation of sandpile formation. Physica A **269**(2–4), 536–553 (1999)